Research

CRISPRi in *Xanthomonas* demonstrates functional convergence of transcription activator-like effectors in two divergent pathogens

Carlos Andrés Zárate-Chaves[1] (iD), Corinne Audran[2] (iD), César Augusto Medina Culma[3] (iD), Aline Escalon[4], Stéphanie Javegny[4], Lionel Gagnevin[1] (iD), Emilie Thomas[1], Léa-Lou Pimparé[1], Camilo E. López[5] (iD), Jonathan M. Jacobs[1,6,7] (iD), Laurent D. Noël[2] (iD), Ralf Koebnik[1] (iD), Adriana Jimena Bernal[3] (iD) and Boris Szurek[1] (iD)

[1]PHIM, Univ Montpellier, IRD, CIRAD, INRAE, Institut Agro, Montpellier 34394, France; [2]LIPME, Université de Toulouse, INRAE, CNRS, Castanet-Tolosan 31326, France; [3]Laboratorio de interacciones moleculares de microorganismos agrícolas (LIMMA), Universidad de los Andes, Bogotá 111711, Colombia; [4]CIRAD, UMR PVBMT, Saint-Pierre 97410, La Réunion, France; [5]Manihot Biotec, Departamento de Biología, Universidad Nacional de Colombia, Bogotá 111321, Colombia; [6]Department of Plant Pathology, The Ohio State University, Columbus, OH 43210, USA; [7]Infectious Diseases Institute, The Ohio State University, Columbus, OH 43210-1358, USA

Authors for correspondence:
Boris Szurek
Email: *boris.szurek@ird.fr*

Adriana Jimena Bernal
Email: *abernal@uniandes.edu.co*

Summary

- Functional analysis of large gene families in plant pathogens can be cumbersome using classical insertional mutagenesis. Additionally, Cas9 toxicity has limited the application of CRISPR–Cas9 for directed mutagenesis in bacteria.
- Here, we successfully applied a CRISPR interference strategy to investigate the cryptic role of the transcription activator-like effector (*tale*) multigene family in several plant-pathogenic *Xanthomonas* bacterial species, owing to their contribution to pathogen virulence.
- Single guide RNAs (sgRNAs) designed against *Xanthomonas phaseoli* pv *manihotis* tale conserved gene sequences efficiently silenced expression of all tales, with concomitant decrease in virulence and TALE-induced host gene expression. The system is readily translatable to other *Xanthomonas* species infecting rice, citrus, Brassica, and cassava, silencing up to 16 tales in a given strain using a single sgRNA. Complementation with plasmid-borne designer *tales* lacking the sgRNA-targeted sequence restored molecular and virulence phenotypes in all pathosystems.
- Our results evidenced that *X. campestris* pv campestris CN08 *tales* are relevant for symptom development in cauliflower. They also show that the MeSWEET10a sugar transporter is surprisingly targeted by the nonvascular cassava pathogen *X. cassavae*, highlighting a new example of TALE functional convergence between phylogenetically distant *Xanthomonas*. Overall, this novel technology provides a platform for discovery and rapid functional understanding of highly conserved gene families.

Introduction

The clustered regularly interspaced short palindromic repeats (CRISPR) and their associated proteins (Cas) or CRISPR–Cas system is an adaptive immunity mechanism present in several bacteria and archaea that protects cells from bacteriophage attack through nucleic acid restriction (Barrangou *et al.*, 2007). The CRISPR locus contains several short DNA segments that come from previous expositions to bacteriophages, which then are transcribed as small RNAs (crRNAs). These crRNAs interact with a trans-activating CRISPR RNA (tracrRNA), which serves as a binding scaffold, and the Cas endonuclease to form an active complex. The Cas nuclease in the complex scans intracellular DNA for a short nucleotide motif called protospacer-adjacent motif (PAM), which is positioned between two protein domains present in the nuclease lobe. This interaction unfolds the target DNA, and the crRNA in the complex is exposed to test the sequence complementarity. Once the Cas nuclease interacts with the correct PAM, and the crRNA binds to the target sequence, the enzyme cleaves the target nucleic acid (Brouns *et al.*, 2008; Gasiunas *et al.*, 2012). Besides the successful implementation of this technology for genome editing in eukaryotes and some prokaryotes, modifications, and additions of protein domains to the Cas9 nuclease have increased the application range for these systems. Translational fusions of cleavage-deficient Cas9 mutant variants to deaminases, transcriptional repressors/activators, histone modification enzymes, and fluorescent proteins enable base editing, gene expression control, epigenetic regulation, and high-resolution spatial imaging, among others (Liu *et al.*, 2021).

Until recently, CRISPR-based genome editing in eukaryotes was achieved upon double-strand break (DSB) of the target DNA and repaired by the host. A homologous template sequence with the desired DNA alteration can also be provided to induce precise insertions through the homology-directed repair (HDR) pathway, although these templates are often associated with cellular toxicity. In the absence of a homologous template, the error-prone, nonhomologous end joining (NHEJ) DNA repair mechanism results in insertions and/or deletions (indels) in the repaired position. However, new technological variants allow editing in absence of NHEJ and HDR pathways in the host (Anzalone et al., 2020). By contrast, most bacteria lack NHEJ systems, and Cas9 activity results in lethality due to unresolved chromosomal breaks in these organisms (Cui & Bikard, 2016). The use of catalytically impaired variants of Cas9 allowed the development of DSB-free gene editing and gene silencing technologies that work in bacteria. nCas9, a catalytically impaired variant of Cas9 inducing nick formation, can be fused to a deaminase and induce cytosine-to-thymine or adenine-to-guanine substitutions (Gaudelli et al., 2017), or be fused to a reverse transcriptase to create template-based insertions in situ (Anzalone et al., 2019). dCas9, a catalytically dead variant of Cas9, per se preserves its PAM specificity and the complex formed with the single guide RNA (sgRNA, a small RNA where the crRNA and the tracrRNA are fused through a short nucleotide loop for biotechnological purposes) can bind specifically to the target DNA, leading to sgRNA-guided Cas9 protein complex positioning. This interaction can interfere with transcription initiation or elongation, resulting in the silencing of the target gene in a process known as CRISPR interference (CRISPRi; Bikard et al., 2013; Qi et al., 2013). CRISPR interference reduces transcription rates by physically interfering with RNA polymerase and/or transcription factors. When the sgRNA targets any of the strands of the promoter region, the dCas9/sgRNA complex sterically prevents the association between the trans-acting transcription factors and their corresponding DNA elements. When the sgRNA targets the nontemplate strand of the coding region, RNA polymerase progression is blocked by the association between the dCas9/sgRNA complex and the DNA (Qi et al., 2013).

Transcription activator-like effector (tale) genes belong to a large family of virulence factors conserved in most species of the plant-pathogen genus Xanthomonas (Schandry et al., 2018). The number of tale genes in a single genome (TALome) varies from 0 to almost 30; most pathovars harbor 1–5 tale paralogs, while some Xanthomonas oryzae pv oryzicola (Xoc) strains have up to 29 (Schandry et al., 2018). Except for Xanthomonas oryzae pv oryzae (Xoo) and Xoc where all described tale genes are chromosomal, tale genes are often encoded on plasmids or plasmid-borne chromosomal insertions (Erkes et al., 2017; Schandry et al., 2018), where transposition and horizontal gene transfer play key roles in tale gene multiplication and evolution (Ferreira et al., 2015). TALE proteins are delivered to plant host cytoplasm through the type three secretion system (T3SS). The particular structure of these effectors allows them to specifically bind host DNA sequences in promoters to induce transcription of downstream genes. TALE proteins are composed of an N-terminal region containing the signal for T3SS-mediated translocation, while the C-terminus holds two to three nuclear localization signals and an acidic transcriptional activation domain responsible for RNA polymerase recruitment (Boch & Bonas, 2010; Perez-Quintero & Szurek, 2019). The central region is characterized by the arrangement of a variable number of tandem modular repeats of 33–35 amino acids. Each repeat has two variable residues at positions 12 and 13, referred to as repeat variable di-residue (RVD), which binds to a DNA base in the target sequence (Boch et al., 2009; Moscou & Bogdanove, 2009). The central region wraps around the DNA in a right-handed superhelix, and the RVD sequence of the repeats governs the target DNA recognition (Mak et al., 2012). Usually, this target sequence, known as the effector-binding element (EBE), is in the vicinity of the transcription start site and is often close to the TATA box. Upon DNA binding, TALEs interact with the gamma subunit of the general transcription factor TFIIA to induce polymerase II-dependent transcription of the downstream gene (Yuan et al., 2016).

TALEs play important roles in the virulence and avirulence of many Xanthomonas species by activating the transcription of host susceptibility (S) genes that confer fitness advantages to the pathogen, or executor (E) genes that act like molecular traps and induce plant cell death. Disruption of major virulence tale genes, that is, those that activate S genes transcription, results in a dramatic reduction of pathogen aggressiveness and/or virulence, as reported for several pathosystems such as Xoo-Oryza sativa (rice), Xanthomonas phaseoli pv manihotis (Xpm)-Manihot esculenta (cassava), and Xanthomonas citri pv citri (Xci)-Citrus (Perez-Quintero & Szurek, 2019). Most of the S genes discovered so far can be grouped into two main functional categories: transcriptional master regulators and nutrient release systems (Xue et al., 2021). Within the last category, TALE-mediated activation of sugars will eventually be exported transporters (SWEET) genes is a conserved strategy shown to support water soaking and bacterial growth during Xanthomonas colonization of rice, cotton, and cassava (Breia et al., 2021). In cassava, several variants of TALE20 activate transcription of the key S gene MeSWEET10a (Zárate-Chaves et al., 2021b).

In this study, we evaluated CRISPRi-mediated silencing for the functional analysis of gene families in Xanthomonas using tale gene family as a proof of concept. We show that sgRNAs targeting regulatory functional elements conserved in the promoter and 5'-UTR regions of tale genes of the cassava pathogen Xpm successfully reduced tale gene expression. We demonstrate that complementation with an sgRNA-resistant plasmid-borne tale gene restores wild-type (WT)-like molecular and pathogenic phenotypes. Moreover, the tool was applied to strains of Xoo, Xci, X. campestris pv campestris (Xcc), and X. cassavae (Xc), successfully silencing full tale gene repertoires in all these different pathogens. Pathogenicity assays with Xoo and Xc confirmed the crucial role of the tale gene family in Xoo and evidenced for the first time its role in Xc virulence on cassava. Overall, we demonstrate that the CRISPRi-dCas9 is a powerful strategy for forward genetic analyses of gene families in Xanthomonas, with potential applicability to other bacterial taxa.

Materials and Methods

Detailed methods are described in the Supporting Information Methods S1.

Bacterial strains, media, and culture conditions

The bacterial strains and culture conditions used in this study are detailed in the Supporting Information. *Xpm* strains were grown on YPG; *Xoo*, *Xci*, and *Xc* strains were grown on PSA, and *Xcc* strains were grown on MOKA. Media composition is described in Methods S1. Media were supplemented with cycloheximide, gentamicin, and/or tetracycline when needed, and all strains were grown at 28°C.

Genome sequencing and *tale* promoter sequence retrieval

Sequenced strains are listed in Table S1. Genomic DNA was extracted with Genomic-tip 100/G (Qiagen) and used to construct 20-kb Pacific Biosciences libraries, which were sequenced with the Sequel platform. Genomes were assembled with CANU v.1.8 (Koren *et al.*, 2017) and CIRCLATOR v.1.5.5 (Hunt *et al.*, 2015), and polished with ARROW (Chin *et al.*, 2013). *tale* genes were annotated with ANNOTALE v.1.2 (Chin *et al.*, 2013), and genomes were explored with GENEIOUS PRIME® 2022.0.2 (Biomatters Ltd, Boston, MA, USA). Annotated RefSeq genomes for PXO99[A], MAI1, and IAPAR 306 were retrieved from NCBI under accession nos. CP000967.2, NZ_CP025609.1, and AE008923.1, respectively.

Design of sgRNAs, CRISPRi plasmid construction, and chromosomal insertion

Two potential crRNAs were designed to be complementary to the nontemplate strand of the *Xpm tale* promoter for CRISPRi (Fig. S1) according to Doench and coworkers for in-target activity (Doench *et al.*, 2014) and to Hsu and coworkers for the off-target scoring method (Hsu *et al.*, 2013). The two crRNAs were aligned to the *Xoo* MAI1, *Xoo* PXO99[A], *Xci* IAPAR 306, *Xcc* CN08, and *Xc* CFBP 4642 *tale* promoters to predict the silencing effectiveness (Fig. S2). Designed crRNAs were synthesized as single-stranded oligonucleotides (Table 1) and directionally cloned into pENTR/D TOPO pgRNA *Bsa*I:*Bsa*I (Figs S3, S4), which contains the J23119 promoter, the Cas9-handle, and a terminator. Each sgRNA scaffold was then transferred to the pUC18-mini-Tn7T-Gm-Gw-dCAS9 through a recombination reaction using the Gateway™ LR Clonase™ II Enzyme Mix (Thermo Fischer Scientific, Waltham, MA, USA), according to manufacturer's instructions. pENTR-GUS (Thermo Fischer Scientific) was used to create a control, where the sgRNA scaffold was replaced by the promoterless *uidA* gene. Plasmids were verified by restriction digest, PCR, and Sanger sequencing. The resulting plasmids were co-electroporated with pTNS1 (containing the Tn7t machinery) into *Xanthomonas* competent cells to obtain targeted chromosomal insertions. Detailed protocols are described in Methods S1.

Poly-*tale* mutant, dTALE, and TALE-expressing vector construction and transformation

Xci IAPAR 306 *tale* genes were deleted by double homologous recombination based on sequence specificities of *tale*-flanking regions. The protocol is detailed in Methods S1. The *MeSWEET10a*-activating dTALE used in this study was designed as in Cohn *et al.* (2014) and is identified as dT*MeSWEET10a*-4. The *OsSWEET14*-activating dTALE was designed as in Streubel *et al.* (2013) and identified as artTAL14-2. dTALEs were built through Golden TAL Technology in the pSKX1 vector as described (Geißler *et al.*, 2011). The *MeSWEET10a*-activating dTALE was transferred to the expression vector pME6010 by restriction ligation using *Hind*III (NEB, Ipswich, MA, USA) and *Bgl*II (NEB; Fig. S4). Transformation of Xam668, PXO99[A], and CFBP 4642 CRISPRi strains was achieved by electroporation.

Plant material, culture conditions, and pathogen inoculation

Plants of cassava (*Manihot esculenta* Crantz) cultivars 60444 and CM6438-14, rice (*Oryza sativa* L ssp. *japonica*) cultivar Kitaake, sweet orange (*Citrus sinensis* (L.) Osbeck) cultivar Valencia, and cauliflower (*Brassica oleracea* var. *botrytis* L) cultivar Clovis (Vilmorin) were grown in glasshouses (see Supporting Information for details). *Xpm*-induced water-soaking symptoms were assessed on leaves of 6-wk-old cassava plants from the 60444 cultivar, while CM6438-14 cultivar was used for *Xc* infections. Bacterial suspensions of *c.* 2×10^8 CFU ml^{-1} in 10 mM MgCl$_2$ were infiltrated through the abaxial surface. Infiltrated points were photographed at 4 d postinoculation (dpi; for *Xpm*) or 5 dpi (for *Xc*) under a stereoscope. *Xpm* growth was assessed by plate count at 0 and 7 dpi after infiltration of *c.* 2×10^6 CFU ml^{-1} in 60444 cassava leaves. Three plants were used per experimental set.

Xoo-induced lesions were assessed in 4-wk-old Kitaake rice plants by leaf-clipping with bacterial suspensions of *c.* 2×10^8 CFU ml^{-1}, and symptom lengths were measured at 15 dpi. *Xoo*-induced water-soaking symptoms were assessed in 3-wk-old plants by infiltration with bacterial suspensions of *c.* 2×10^8 CFU ml^{-1}. Photographs were taken at 4 dpi. *Xci*-induced symptoms were assessed in mature fully expanded leaves of sweet orange plants from the cultivar Valencia. Leaves were syringe-infiltrated with bacterial suspensions of *c.* 1×10^8 CFU ml^{-1}, scanned, and photographed from 7 to 13 dpi. Symptoms caused by *Xcc* in 4-wk-old cauliflower plants were assessed by wound inoculation in the midvein with bacterial suspensions of *c.* 10^8 CFU ml^{-1}; disease was assessed by a disease score at 10 dpi (Table S2). All assays were replicated at least three times. Additional details on inoculation protocols are included in Methods S1.

TALE protein expression assays

Total protein extracts in 1× Laemmli buffer were separated on 7.5% Mini-Protean® TGX Gel (Bio-Rad) by SDS-PAGE. The transfer to a nitrocellulose membrane was carried out in the Transblot turbo (Bio-Rad), using the integrated protocol HIGH

Table 1 CRISPR RNAs (crRNAs) used to construct the single guide RNAs (sgRNAs) for *tales* silencing.

crRNA	Targeted region[a]	Sequence	PAM	Activity score[b]	Off-target score (%)[c]
−10−35	−55 : −36	GACCAGAGATCTTTTAGTCT	TGG	0.029	100.00
RBS	−19 : +1	CTATAAAGAGGTATGCCTGA	TGG	0.583	100.00

Both crRNAs are complementary to the nontemplate (Watson) strand. PAM, protospacer-adjacent motif; RBS, ribosome-binding site.
[a]Position is relative to the first nucleotide of the coding sequence (numbered as +1).
[b]Calculated in GENEIOUS PRIME® 2022.0.2 with the algorithm proposed by Doench *et al*. (2014).
[c]Calculated in GENEIOUS PRIME® 2022.0.2 with the algorithm proposed by Hsu *et al*. (2013).

MW. Polyclonal rabbit anti-TALE primary antibodies directed against *Xoo* (Read *et al*., 2016) or *Xcc* TALE (L. D. Noël and Ivanna Fuentes, unpublished) and a secondary anti-rabbit HRP (HorseRadish Peroxidase)-conjugated antibody were used to detect TALEs by chemiluminescence using Clarity ECL Reagent (Bio-Rad) and the Bio-Rad Chemidoc Imager according to the manufacturer's instructions. The detailed protocol is included in Methods S1.

Infiltration, RNA extraction, and retro-transcriptase quantitative PCR (RT-qPCR)

Xpm or *Xci* suspensions of *c*. 5×10^8 CFU ml^{-1} (in 10-mM MgCl$_2$) were infiltrated into the abaxial surface of 4-wk-old cassava leaves or fully expanded sweet orange leaves, respectively. Infiltrated tissue was collected at 50 hpi and ground in liquid nitrogen in a TissueLyser II (Qiagen). Total cassava RNA was extracted using the Invitrap Spin plant RNA Mini Kit (Stratec, Birkenfeld, Germany) per the manufacturer's instructions. Sweet orange RNA was extracted with the TRIzol reagent (Thermo Fisher Scientific) according to the manufacturer's instructions. Total RNAs were treated with TURBO™ DNase (Thermo Fisher Scientific), and cDNA synthesis was performed with the SuperScript™ III Reverse Transcriptase (Thermo Fisher Scientific) and an Oligo(dT)12–18 Primer (Thermo Fisher Scientific). RT-qPCRs were performed with the Eurogentec Takyon™ SYBR® 2× qPCR Mastermix Blue (Sycamore Life Sciences, Houston, TX, USA) containing 0.3 μM of each primer in a LightCycler® 480 System (Roche Life Science). PCR cycling was as follows: 95°C for 10 min, followed by 40 cycles of 95°C for 15 s, and 60°C for 30 s. Table S3 lists the primers used in this study, and the Methods S1 includes more details on the protocols used.

TALE target prediction analysis

TALE targets were predicted using TALVEZ (Pérez-Quintero *et al*., 2013) on the cassava promoterome (1-kb sequences preceding annotated translational start sites) extracted from PHYTOZOME's cassava genome v.6.1 (Bredeson *et al*., 2016). The algorithm was run using the default parameters. Output data were analyzed in R (v.3.6.1) using an in-house script.

Statistical analyses

Analyses were performed in R (v.3.6.1). Most of the datasets were analyzed through linear mixed models (repetitions of the whole experiment were used as random effect) coupled to *post hoc* Tukey's test with a confidence level of 95%. Disease scores were analyzed through a Kruskal–Wallis test coupled to a *post hoc* Dunn's test with Benjamini–Hochberg's correction.

Results

Establishment of a CRISPR-based silencing platform in *X. phaseoli* pv *manihotis* allows efficient *tale* gene knockdown

In order to knockdown the greatest number of *tale* genes within and across strains of the cassava bacterial blight pathogen *X. phaseoli* pv *manihotis* (*Xpm*) using a single sgRNA, we searched for conserved sequences across *tale* promoters and 5′UTR sequences. To this end, we sequenced the genome of 10 *Xpm* isolates collected world-wide (Table S1) from which we extracted 31 *tale* gene sequences (Table S4). Promoter sequences were aligned and scanned for potential N(20)NGG crRNAs. Two crRNAs directed against the nontemplate strand were selected, one targeting the −10 and −35 element region, and a second one targeting the ribosome binding site (Figs 1a, S1). The −10 and −35 element was conserved across the 31 sequences. For the RBS crRNA, there were two polymorphisms at positions +13 and +14 present in 12 out of the 31 ribosome-binding site (RBS) sequences. The selected crRNA reflects the most frequent sequence. Because the specificity is mainly dictated by the first 12 nucleotides, these polymorphisms are not expected to affect activity (Larson *et al*., 2013). As indicated in Table 1, none of the two crRNAs are predicted to have off-targets. Each construct comprises the sgRNA scaffold, dCas9, and the gentamicin resistance expression cassette, all of which is framed by Tn7 borders to allow transposition into the bacterial chromosome (Fig. S4a). As a control to demonstrate that *dCas9* and gentamicin resistance genes do not affect the *in vitro* and *in planta* performance of bacteria, the sgRNA scaffold was replaced by a promoterless *uidA* gene. The construct used for *tale* trans-expression in the knocked-down strains is presented in Fig. S4(b).

To test our silencing platform, we used *Xpm* strain Xam668 whose TALome was characterized by insertional mutagenesis (Cohn *et al*., 2014). Each construct was inserted through Tn7-mediated transposition in a unique locus located downstream of the bacterial-conserved and essential *glmS* gene (Peters & Craig, 2001; Choi & Schweizer, 2006). We first verified that insertion of *dCas9* and gentamicin resistance gene in this locus does not alter growth and virulence of *Xpm* (Fig. S5). TALE
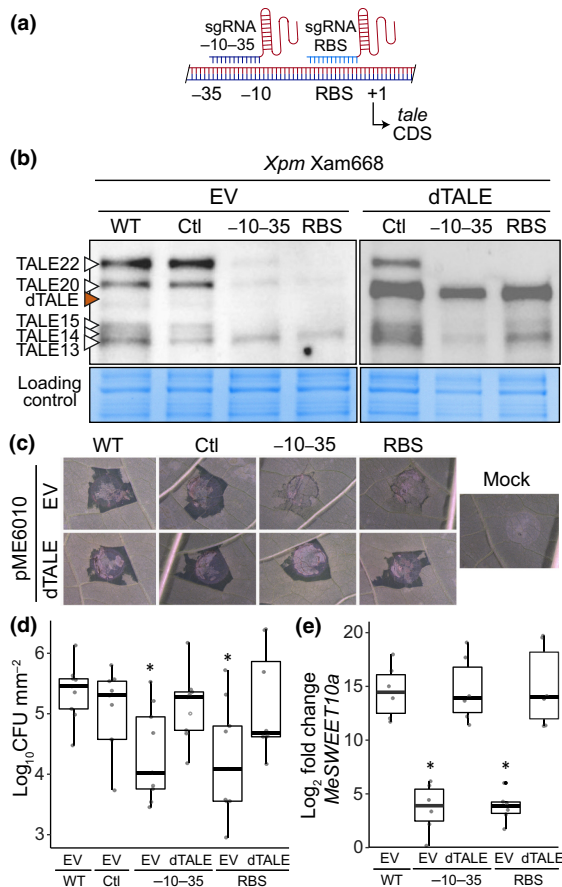
Fig. 1 *Xanthomonas phaseoli* pv *manihotis* (*Xpm*) CRISPRi strains knocked down for *tale* genes are less virulent and can be complemented in protein expression and virulence with a synthetic single guide RNA (sgRNA)-resistant dTALE. (a) Scheme of sgRNAs targeting *Xpm tale* promoters. Double-stranded DNA is represented by the red (nontemplate strand) and blue (template strand) ladder. Positive numbering begins at the start codon. RBS, ribosome-binding site; CDS, coding DNA sequence. (b) Western blot analysis of *Xpm* total protein extracts resolved by SDS-PAGE using anti-TALE antibodies. Wild-type (WT) Xam668 and its CRISPRi derivatives (Control -Ctl-, $-10-35$ and RBS) transformed with pME6010-empty vector (EV) or pME6010-dTALE-SW10A (dTALE) were analyzed. The upper panel shows chemiluminescent signals (anti-TALE) in the western blot assay, while the lower panel shows protein loading by Coomassie blue staining. White arrowheads point to TAL13$_{Xam668}$, TAL14-$_{Xam668}$, TAL15$_{Xam668}$, TAL20$_{Xam668}$, and TAL22$_{Xam668}$ bands, while red arrowhead points to the dTALE band. (c) Water-soaking symptoms at 96 h postinoculation (hpi) in cassava (*Manihot esculenta*) cultivar 60444. Photographs are representative of three biological replicates in the same experimental setup. The whole experiment was repeated four times with similar results. (d) Bacterial titers at 7 d postinoculation on the cassava cultivar 60444 infiltrated with the WT and CRISPRi-derivative strains. Bacterial titers from three replicates of the experimental set ($n = 9$) were analyzed through a linear mixed model. Asterisks indicate significant differences to the WT-EV treatment (Tukey's test: $\alpha = 0.05$). (e) Relative expression of *MeSWEET10a* at 50 hpi with the transformed WT and CRISPRi strain derivatives. Relative expression data from two replicates of the experimental set ($n = 6$) were analyzed through a linear mixed model. Asterisks indicate significant differences to the WT-EV treatment (Tukey's test: $\alpha = 0.05$). Points over the boxplots represent individual observations. The line across the box indicates the median, while upper and lower edges indicate the 25th and 75th percentiles. Whiskers are extended to show the minimum and maximum values. Complete one-to-one *post hoc* comparisons for (d,e) are shown in Supporting Information Fig. S9(a,b).

protein expression was assessed by Western blot analysis using a polyclonal antibody developed against an artificial TALE (Read *et al.*, 2020), which cross-reacts with most of the *Xanthomonas* TALEs, including *Xpm* TALEs (Figs 1b, S6a, S7). Xam668 strain WT and Xam668 strain harboring the promoterless *uidA* gene in place of the sgRNA scaffold (from now on referred to as Xam668-Control) had similar accumulation of the five Xam668 TALEs (TAL13$_{Xam668}$, TAL14$_{Xam668}$, TAL15$_{Xam668}$, TAL20-$_{Xam668}$, and TAL22$_{Xam668}$). By contrast, the strains harboring constructs $-10-35$ and RBS (Xam668-10-35 and Xam668-RBS, respectively) accumulated significantly less TALE proteins. Concomitantly, Xam668-10-35 and Xam668-RBS were unable to induce water-soaking symptoms 96 h postinoculation (hpi) on leaves of the susceptible cassava cultivar 60444 (Figs 1c, S6b), in contrast to Xam668-WT and Xam668-Control.

We next investigated whether the induction of *MeSWEET10a*, an essential *S* gene for *Xpm*, would be sufficient to trigger disease in a context where no other *S* gene can be activated due to *tale* family knockdown. To this end, we used the previously reported synthetic *MeSWEET10a*-activating designer TALE dT*MeSWEET10a*-4 (Cohn *et al.*, 2014), which was expressed under the control of *lac* promoter (Geiβler *et al.*, 2011) to avoid gene trans-knockdown from the CRISPRi construct (from now on dTALE-SW10A). dTALE-SW10A was highly expressed in strains subjected to CRISPRi, while endogenous TALEs are barely detectable (Fig. 1b). Interestingly, induction of *MeS-WEET10a* resulted in the restoration of water-soaking symptoms (Fig. 1c). Accordingly, bacterial titers at 7 dpi of Xam668-10-35 and Xam668-RBS strains transformed with pME6010-EV were lower ($P < 0.05$) than those for Xam668-WT and Xam668-Control, while the CRISPRi strains transformed with the dTALE-SW10A grew at levels that were similar to the ones observed for Xam668-WT and Xam668-Control strains (Fig. 1d). As expected, qRT-PCR expression analysis shows that silencing of TAL20$_{Xam668}$ results in the loss of *MeSWEET10a* upregulation, while dTALE-SW10A restored it (Fig. 1e). Altogether, these data evidence that the CRISPRi silencing platform implemented in *Xpm* is useful for the study of gene families and the relative role of each of its members.

Efficient CRISPRi-based silencing of *Xanthomonas oryzae* and *Xanthomonas citri tale* genes

To further evaluate the potential of CRISPRi for *tale* gene silencing in other *Xanthomonas* species, we knocked down the *tale* gene repertoires of *Xoo* strains PXO99^A and MAI1 (representatives of the Asian and African lineages, respectively), and *Xci* reference strain IAPAR 306, the causal agents of rice bacterial leaf blight (BLB) and Asiatic citrus canker (ACC), respectively (Table S1). The alignment of the *tale* promoter sequences with the designed crRNAs predicted that 35 out of the 38 investigated *tale* genes could be targeted by the RBS crRNA, while $-10-35$ crRNA was less conserved (Table 2; Fig. S2). Interestingly, the entire TALomes of *Xoo* MAI1 (9 *tale* genes) and *Xci* IAPAR 306 (4 *tale* genes) are predicted to be silenced, while three out of 19 *tales* from PXO99^A would be protected against the sgRNA

Table 2 Characterization of the selected CRISPR RNA (crRNA) ribosome-binding site (RBS) against *tales* from other *Xanthomonas* species: *Xanthomonas oryzae* pv *oryzae* (*Xoo*), *Xanthomonas citri* pv *citri* (*Xci*), *Xanthomonas campestris* pv *campestris* (*Xcc*), and *Xanthomonas cassavae* (*Xc*).

Xanthomonas spp.	*tale* ID	M5[a]	M12[b]	M20[c]	Target potential
Xoo MAI1	*talA, talB, talE, talF, talG, talI*	0	0	1	High
	talC, talD, talH	0	0	2	High
Xoo PXO99[A]	*tal1 (pthXo7), tal2a, tal2b (pthXo1), tal4, tal5a, tal5b (pthXo6), tal6a, tal6b, tal7a, tal7b, tal8a, tal8b, tal9a, tal9b (avrXa23), tal9d, tal9e*	0	0	2	High
	tal9c (avrXa27), tal3a, tal3b	1	1	3	Low
Xcc CN08	*tal15e, tal18a, tal22a*	0	0	1	High
	tal12a	0	0	2	High
Xc CFBP 4642	*tale14_{CFBP 4642}, tale15A_{CFBP 4642}, tale15B_{CFBP 4642}, tale16_{CFBP 4642}, tale17_{CFBP 4642}, tale23_{CFBP 4642}*	0	0	2	High

[a]Number of mismatches in the seed sequence (five base pairs adjacent to the protospacer-adjacent motif (PAM)).
[b]Number of mismatches in the first 12 nucleotides.
[c]Number of mismatches over the whole crRNA sequence.

because of one mismatch in the first nine nucleotides, also named seed sequence (Fig. S2).

TALE protein accumulation in the *Xoo* and *Xci* strains transformed with the RBS sgRNA was dramatically reduced (Fig. 2a). Leaf-clip inoculation of both MAI1-RBS and PXO99[A]-RBS strains in the susceptible Kitaake cultivar resulted in a remarkable reduction of lesion lengths at 15 dpi when compared to the WT and Control strains (Fig. 2b). The extent of water-soaked lesions was strikingly reduced to the inoculation point for the RBS strain, while WT and Control strains showed enhanced water soaking beyond the inoculation points (Fig. 2d). We next investigated whether induction of the major BLB susceptibility gene *OsSWEET14* would be sufficient to restore virulence, in a context where most *Xoo tales* are silenced. To that end, we expressed the *OsSWEET14*-activating designer TALE artTAL14-2 (Streubel *et al.*, 2013) under the control of *lac* promoter (from now on dTALE-SW14). dTALE-SW14 is protected against the RBS sgRNA, in PXO99[A] strains undergoing CRISPRi. Our data show that *OsSWEET14* induction leads to a significant but partial restoration of virulence, indicating that other TALE-dependent host targets are required to reach WT-like disease symptoms (Fig. 2c). In parallel, we evaluated whether *tale* gene silencing in *Xci* would also result in reduced canker symptoms in sweet orange. As shown in Fig. 2(e), canker and water soaking were well-developed 9 d after inoculation of leaves of sweet orange plants of the cultivar Valencia with *Xci* strains IAPAR 306 WT

and IAPAR 306-Ctl, which expresses the dCas9 but no sgRNA. By contrast, both symptoms were strongly reduced when sweet orange leaves were infiltrated with *Xci* strain IAPAR 306-RBS and the IAPAR 306 poly-*tale* gene mutant (Δ*tales*; Fig. 2e), resulting in a dramatic reduction of the transcription of the major ACC susceptibility gene *CsLOB1* (Figs 2f, S9; Hu *et al.*, 2014). Altogether, our results show that the *tale* gene silencing platform can be used as a generic tool in several *Xanthomonas* species allowing to test for the contribution of *tale* genes to pathogen virulence.

TALE knockdown highlights a major role in *X. campestris* virulence

We next evaluated the contribution of *tales* to the virulence of *Xanthomonas campestris* pv *campestris* (*Xcc*), the causal agent of black rot disease of *Brassica* crops. Previous characterization of *Xcc* TALome in strain CN08 revealed that it expresses four TALEs (Denancé *et al.*, 2018). The alignment of the *tale* gene promoters for this pathogen showed that the RBS crRNA-binding site is highly conserved and predicted to be functional for silencing *Xcc tales* (Fig. S2). Western blot analysis demonstrated that TALE protein accumulation was dramatically decreased for all the TALEs of strain CN08-RBS (Fig. 3a). Pathogenicity assays highlighted that the virulence of *Xcc* CN08-RBS is reduced, as shown by lower disease scores and milder symptoms on cauliflower (Fig. 3b,c), thus demonstrating the role of TALEs for the pathogenicity of *Xcc* strain CN08.

A novel cassava susceptibility *SWEET* gene for the nonvascular pathogen *X. cassavae*

Xanthomonas cassavae (*Xc*) is the causal agent of cassava bacterial necrosis (CBN), a foliar disease (Zárate-Chaves *et al.*, 2021a). Knowledge on this bacterium is scarce and pathogenesis-related determinants are totally unknown. To test for *tale* gene presence, we resequenced the genome of strain CFBP4642 using a long-read sequencing technology and identified seven of these genes (Table S5). As for the other tested *Xanthomonas*, the RBS crRNA-binding site on *tale* gene promoters is highly conserved (Fig. S1). Knockdown of *tales* in *Xc* resulted in more scattered water-soaked areas and slower symptom development (Figs 4a,b, S8). This finding prompted us to search for candidate cassava genes targeted by *Xc* TALEs, using the Talvez program which predicts EBEs in a host genome based on the TALE code (Pérez-Quintero *et al.*, 2013; Table S6). Strikingly, TALE23 is predicted to target the CBB susceptibility gene *MeSWEET10a* known to be induced by *Xpm* TAL20 upon binding to a 20-nt EBE, which is overlapping with that predicted for TALE23 (Fig. 4d). To assess the role of *MeSWEET10a* in CBN, CRISPRi *Xc* strains were transformed with the pME6010-dTALE-SW10A or the EV and leaf-infiltrated into CM6438-14 cassava plants. Water-soaked symptoms were restored upon the expression of dTALE-SW10A and correlated with *MeSWEET10a* upregulation in the leaves at 48 hpi (Fig. 4b,c). This is the first description of the molecular mechanisms underlying the pathogenicity of the nonvascular

(a)

(b) **(c)**

(d) *Xoo* MAI1

WT Ctl RBS Mock

(e) *Xci* IAPAR306 **(f)**
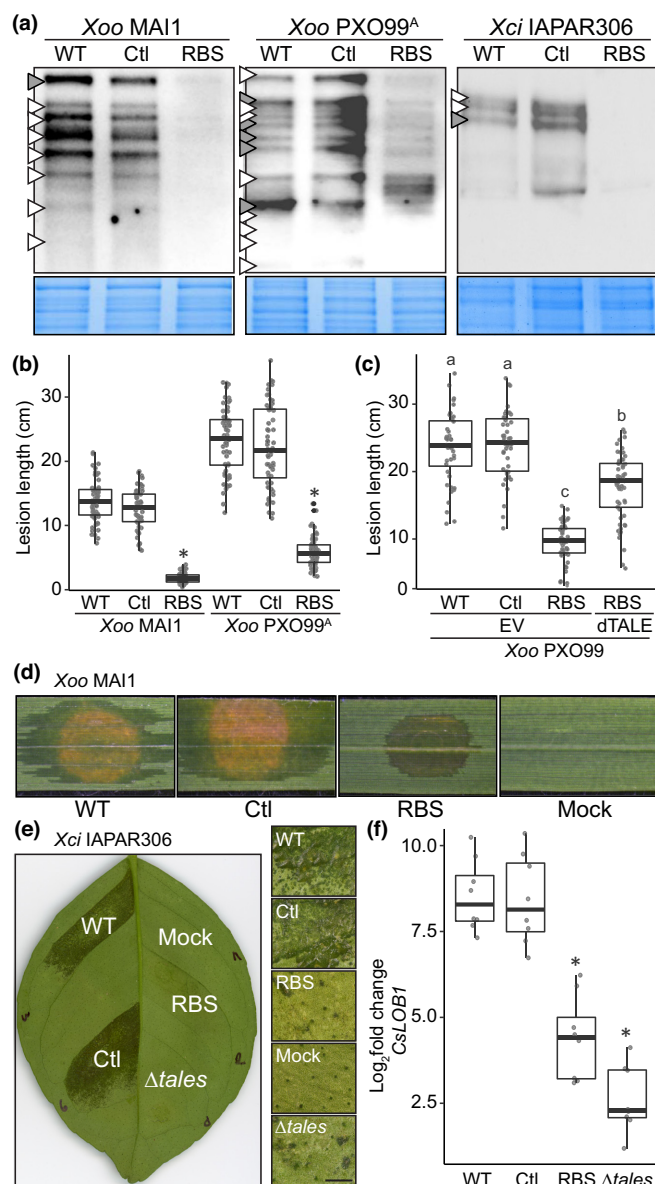
Fig. 2 *tale* gene silencing in *Xanthomonas oryzae* pv *oryzae* (*Xoo*) and *Xanthomonas citri* pv *citri* (*Xci*) dramatically reduces disease symptoms. (a) Western blot analysis of *Xanthomonas* total protein extracts resolved by SDS-PAGE using anti-TALE antibodies. Wild-type (WT) *Xoo* MAI1 and PXO99[A], and *Xci* IAPAR 306 strains, and their CRISPRi derivatives (Control -Ctl- and ribosome-binding site (RBS)) were analyzed. The upper panel shows chemiluminescent signals (anti-TALE) in the western blot assay, while the lower panel shows protein loading by Coomassie blue staining. White arrowheads point to TALE bands; gray arrowheads point to bands with two TALEs with similar theoretical molecular weights (Supporting Information Fig. S7). (b) Lesion lengths caused by the *Xoo* WT and CRISPRi-derivative strains at 15 d postinoculation (dpi) on Kitaake rice (*Oryza sativa*) plants. Lesion length data from three replicates of the experimental set (*n* > 54) were analyzed through a linear mixed model. Asterisks indicate significant differences to the WT treatment (Tukey's test: α = 0.05). (c) Lesion lengths caused by the WT and CRISPRi *Xoo* PXO99[A] strains transformed with the empty vector (EV) or the *OsSWEET14*-inducing dTALE-SW14 (dTALE). Symptoms were measured at 15 dpi on Kitaake rice plants. Lesion length data from three replicates of the experimental set (*n* > 44) were analyzed through a linear mixed model. Different letters indicate significant differences among treatments (Tukey's test: α = 0.05). (d) Representative photos of water-soaking symptoms caused by the WT and the CRISPRi MAI1 strains in Kitaake rice leaves at 72 h postinoculation (hpi). (e) Representative photographs of cankers and water-soaking symptoms caused by the *Xci* IAPAR 306 WT and CRISPRi strains on Valencia sweet orange (*Citrus sinensis*) leaves at 9 dpi. Panels on the right show a magnification of the inoculated tissues. Bar, 1 mm. (f). Relative expression of *CsLOB1* at 50 hpi of the *Xci* IAPAR 306 WT strain, CRISPRi strain derivatives (Control -Ctl- and RBS) and an IAPAR 306 poly-*tale* derivative mutant strain (Δ*tales*). Relative expression data from three replicates of the experimental set (*n* = 8) were analyzed through a linear mixed model. Asterisks indicate significant differences to the WT treatment (Tukey's test: α = 0.05). Points over the boxplots represent individual observations. The line across the box indicates the median, while upper and lower edges indicate the 25th and 75th percentiles. Whiskers are extended to show the minimum and maximum values. Complete one-to-one *post hoc* comparisons for (b,c,f) are shown in Supporting Information Fig. S9(c–e).

pathogen *Xc*. Taken together, our results indicate that the CRISPRi silencing platform is versatile, simple, and efficient for the functional characterization of gene families in *Xanthomonas*.

Discussion

CRISPRi silencing mediated by dCas9 has been successfully used in several bacterial species for functional analysis of genes and pathways, engineering biotechnologically desirable traits, or identifying drug targets (Ding *et al.*, 2020). CRISPR interference platforms have been established in many human and animal pathogens including *Vibrio cholerae*, *Yersinia pestis*, *Streptococcus pneumoniae*, and *Staphylococcus aureus* (Zhang *et al.*, 2021). To the best of our knowledge, such system has never been applied to plant-pathogenic bacteria, while a few examples were reported for plant-associated microorganisms such as *Pseudomonas fluorescens*

(Tan *et al.*, 2018) and *Paenibacillus sonchi* (Brito *et al.*, 2020). Here, we demonstrated the potential of CRISPRi for rapid and efficient knockdown of an entire gene family of major virulence factors from the plant-pathogenic bacterium *Xanthomonas*, applying only one sgRNA which targets a highly conserved sequence in their promoters or 5′-UTR regions. Importantly, no dCas9-associated toxicity could be noted and silencing rates were high enough to result in reduced disease phenotypes in all the *Xanthomonas* species tested here, including *Xcc* and *Xc* where the virulence role of TALEs was less advanced.

Established first for *Xpm*, the CRISPRi-based silencing of *tale* genes was sufficient to significantly reduce the induction of the *S* gene *MeSWEET10a*, resulting in notably decreased water soaking. The restoration of virulence upon complementation of *Xpm* CRISPRi strains with a synthetic TALE targeting *MeSWEET10a* further confirmed the essential role of this sugar transporter during CBB, as previously shown through the characterization of mutant strains inactivated in TAL20 which induces *MeSWEET10a* expression (Cohn *et al.*, 2014). Interestingly, gene silencing was equally potent for all the *tale* genes of *Xpm*, despite the presence of two RBS sequence variants. These results are consistent with the specificity of the dCas9 complex being dictated
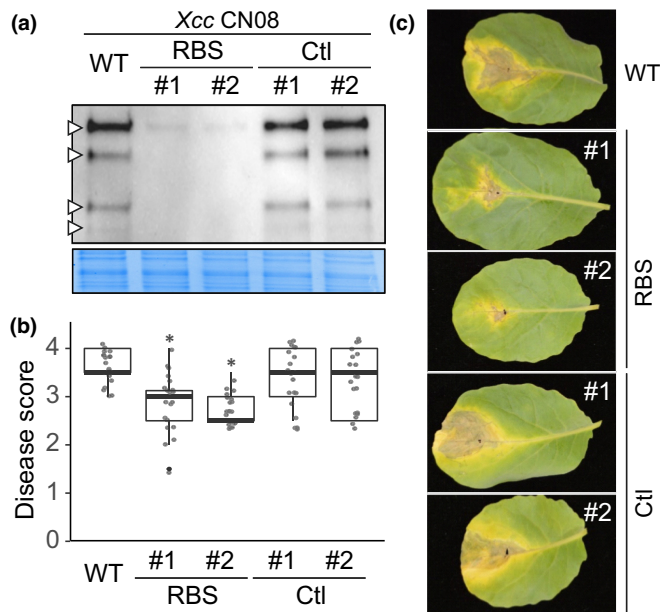
Fig. 3 *Xanthomonas campestris* pv *campestris* (*Xcc*) strains undergoing *tale* knockdown are less virulent on cauliflower (*Brassica oleracea* var. *botrytis*) cultivar Clovis. (a) Western blot analysis of *Xanthomonas* total protein extracts resolved by SDS-PAGE using anti-TALE antibodies. Wild-type (WT) *Xcc* strain CN08 strain, and their CRISPRi derivatives (Control – Ctl – and ribosome-binding site (RBS)) were analyzed. The upper panel shows luminescent signals (anti-TALE) in the western blot assay, while the lower panel shows protein loading by Coomassie blue staining. White arrowheads point to TALE bands (Supporting Information Fig. S7d). Two independent transformants were assessed for TALE expression (#1 and #2). (b) Virulence assessment at 10 d postinoculation for *Xcc* strains inoculated by piercing on cauliflower leaves. Disease was scored in four independent replicates of the experimental set (*n* = 20) and analyzed through a Kruskal–Wallis test. Asterisks indicate significant differences to the WT (Dunn's test with Benjamini–Hochberg's correction: α = 0.05). Points over the boxplots represent individual observations. The line across the box indicates the median, while upper and lower edges indicate the 25th and 75th percentiles. Whiskers are extended to show the minimum and maximum values. Complete one-to-one *post hoc* comparisons for (b) are shown in Supporting Information Fig. S9(f). (c) Representative photographs for the median disease scores of black rot disease symptoms caused by *Xcc* CN08 strain derivatives.

by the first 12 nucleotides of the sgRNA and the two nucleotides of the PAM (Larson *et al.*, 2013). This observation indicates that special attention should be paid to the seed sequence constituted by the first nine nucleotides during sgRNA design (Cui & Bikard, 2016).

Owed to the high level of conservation of their promoter sequences, we were able to extend our knockdown analysis to *Xanthomonas tale* repertoires in four other crop pathogens, namely *Xoo*, *Xci*, *Xcc*, and *Xc*. In all these cases, Western blot analysis revealed that most if not all TALE bands were barely detectable, including those of the *Xoo* strain PXO99^A, whose genome encodes 19 *tale* genes (Salzberg *et al.*, 2008). Regarding this strain, it is noteworthy that dTALE-induced expression of *OsSWEET14*, which is a major BLB *S* gene, was sufficient to overcome most but not all of the virulence defects caused by *tale* silencing. This result is in agreement with previous data showing that PXO99^A relies on the induction of other *S* genes for full virulence. These could include the

transcription factor *OsTFX1,* which is targeted by the TALE PthXo6 (Sugio *et al.*, 2007). Similar conclusions were drawn upon the systematic deletion of all PXO99^A *tale* genes, whereby the deletion of *pthXo1*, which induces *OsSWEET11*, had the strongest impact on virulence (Ji *et al.*, 2016). Silencing of the *Xci* IAPAR 306 strain TALome prevented canker symptoms and dramatically decreased the expression of *CsLOB1*. As expected, *CsLOB1* induction was higher upon infection of sweet orange leaves with the silenced strain IAPAR 306-RBS than with the poly-*tale* mutant, where all *tales* including *pthA4* are knocked out.

In *Xcc* strain CN08, *tale* gene silencing resulted in decreased disease scores in cauliflower. In previous studies, the combined action of *tal12a* and *tal15a* from *Xcc* strain Xca5 was shown to be implicated in symptom development on radish and cauliflower without affecting pathogen multiplication *in planta* (Kay *et al.*, 2005; Denancé *et al.*, 2018). Interestingly, CN08 also expresses the same *tal12a*, but a different *tal15* gene (Denancé *et al.*, 2018). Hence, *tale*-mediated virulence of *Xcc* might rely on partially distinct susceptibility determinants.

Deployment of the CRISPRi system in *X. cassavae* highlighted the usefulness and versatility of this platform, leading to the unexpected discovery of a new example of evolutionary convergence between TALEs of *Xpm* and *Xc*. *Xpm* is a vascular pathogen, likely originating from South America (as for cassava), while *Xc* is a nonvascular pathogen, phylogenetically distant to *Xpm*, that has likely recently emerged as a cassava pathogen in African highlands (Zárate-Chaves *et al.*, 2021a). Here, we demonstrate that despite their different phylogeny and lifestyles *in planta*, pathogenicity of both pathogens relies on the induction of the expression of *MeSWEET10a*, as initially reported for *Xpm* (Cohn *et al.*, 2014). Although direct evidence for induction of *MeSWEET10a* by TALE23 is lacking, its predicted EBE strikingly overlaps with that of *Xpm* TAL20, suggesting that these two TALEs with completely unrelated RVD arrays have evolved independently to activate *MeSWEET10a*. These results suggest that nonvascular pathogens may also be able to hijack sugar transport for optimized plant infection. This is surprising since SWEET sugar transporters were so far only reported as susceptibility determinants of vascular pathogens such as *Xoo*, *Xpm*, and *X. citri* pv *malvacearum*. In these three pathogens, TALEs are involved in water-soaking symptom formation, which is hypothesized to facilitate the entrance and movement of *Xanthomonas* into the apoplast (Streubel *et al.*, 2013; Cohn *et al.*, 2014; Cox *et al.*, 2017). It is theorized that sugar accumulation supports bacterial growth and also alter osmotic potential of the apoplast, creating an aqueous environment (Aung *et al.*, 2018).

The CRISPRi platform presented here allowed the efficient silencing, within a strain, of up to 16 genes from the TALE family using a single sgRNA. Impacts of this accomplishment are highly significant, since the obtention of the equivalent poly-deletion mutant strain through sequential mutagenesis of each individual *tale* gene would have been extremely cumbersome and time-consuming. For example, a *Pseudomonas syringae* DC3000 poly-mutant strain (DC3000D28E) where genes encoding the 28 type three effectors (T3Es) were successively deleted required 4 yr of experimentation (Wei *et al.*, 2007;
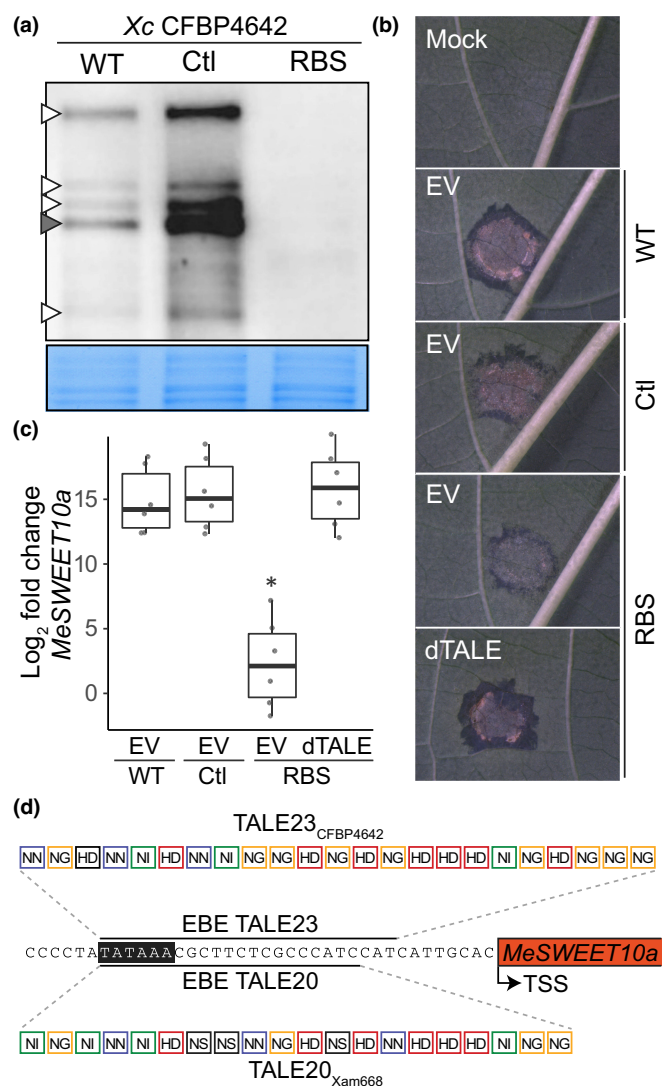
Fig. 4 Nonvascular pathogen *Xanthomonas cassavae* (*Xc*) relies on *tale* genes for full virulence on cassava (*Manihot esculenta*) and for the induction of the expression of *MeSWEET10a* sugar transporter gene. (a) Western blot analysis of *Xc* total protein extracts resolved by SDS-PAGE using anti-TALE antibodies. Wild-type (WT) *Xc* CFBP4642 strain and their CRISPRi derivatives (Control -Ctl- and ribosome-binding site (RBS)) were analyzed. The upper panel shows luminescent signals (anti-TALE) in the western blot assay, while the lower panel shows protein loading by Coomassie blue staining. White arrowheads point to TALE bands; gray arrowheads point to bands with two TALEs with similar theoretical molecular weights (Supporting Information Fig. S7e). (b) Representative photographs of water-soaking symptoms observed at 5 d postinoculation on leaves of cassava cultivar CM6438-14 infiltrated with *Xc* CFBP4642 WT and CRISPRi derivatives transformed with pME6010-empty vector (EV) or pME6010-dTALE-SW10A (dTALE). The whole experiment was repeated three times with similar results (Fig. S8). (c) Relative expression of *MeSWEET10a* in cassava cultivar CM6438-14 leaves at 50 h postinoculation with the WT and the complemented CRISPRi strains. Data from two replicates of the experimental set ($n = 6$) were analyzed through a linear mixed model. Asterisks indicate significant differences to the WT-EV treatment (Tukey's test: $\alpha = 0.05$). Points over the boxplots represent individual observations. The line across the box indicates the median, while upper and lower edges indicate the 25th and 75th percentiles. Whiskers are extended to show the minimum and maximum values. Complete one-to-one *post hoc* comparisons for (c) are shown in Supporting Information Fig. S9(g). (d) Schematic representation of the predicted evolutionary convergence of *Xc* TALE23$_{CFBP4642}$ and *Xanthomonas phaseoli* pv *manihotis* TAL20$_{Xam668}$. Both TALEs are predicted to bind overlapping effector-binding elements (EBEs) in the promoter sequence of *MeSWEET10a* (Manes.06123400). The black-highlighted motif shows a putative TATA box. The red box represents the predicted transcript and TSS stands for transcriptional start site. TALEs are depicted as a string of color-coded boxes that reflect the repeat variable di-residue (RVD) sequences of each effector.

Kvitko *et al.*, 2009; Cunnac *et al.*, 2011). These mutants allowed the discovery of the key defense-eliciting or virulence role of several T3Es in *Nicotiana benthamiana* and tomato. Implementation of CRISPRi with multiplexed sgRNAs may now allow this achievement in a considerably shorter time. Single guide RNA multiplexing has been reported for up to 10 different targets at the same time using an array of crRNAs and spacers controlled by a unique strong promoter (Ellis *et al.*, 2021). Engineered *Streptococcus pyogenes* Cas9 enzymes with more relaxed PAM consensus motifs (Collias & Beisel, 2021) could be exploited in the future to differentially silence gene family members, allowing for more fine-tuned experiments. In conclusion, our study demonstrates the usefulness of the CRISPRi platform to study large gene families in the plant-pathogenic bacterium *Xanthomonas*, and its strong potential to dissect the relevance of functionally redundant genes involved in bacterial pathogenesis. Although this tool is very versatile and easy to apply, attention should be paid to the design, which dictates the limitations of its implementation. Hopefully, further optimization and adaptation of the platform

along with other CRISPR-based technologies such as base editors (Banno *et al.*, 2018), will increase the technology adoption and widen the array of molecular tools for the study of *Xanthomonas* and other bacterial pathogens.

Competing interests

None declared.

Author contributions

CAMC, L-LP, JMJ and RK performed preliminary proof-of-concept tests. CAZ-C carried out all the experiments except for the tests on *X. campestris* pv *campestris*, performed the statistical analysis, and wrote the manuscript. ET propagated the cassava and rice plant material. AE and SJ performed the mutagenesis by double homologous recombination for *X. citri* pv *citri* strain. LG advised on the *X. citri* pv *citri* experiments and provided the plant material for sweet orange assays. CA and LDN designed, performed, and analyzed all the experiments on *X. campestris* pv *campestris*. CA performed all the Western blots displayed in this article. CEL, RK, AJB and BS participated in the experimental design and conception of the study. All the coauthors reviewed and corrected the manuscript.

ORCID

Corinne Audran https://orcid.org/0000-0002-3083-8088
Adriana Jimena Bernal https://orcid.org/0000-0002-3557-697X
Lionel Gagnevin https://orcid.org/0000-0002-2943-0827
Jonathan M. Jacobs https://orcid.org/0000-0002-1553-2013
Ralf Koebnik https://orcid.org/0000-0002-4419-0542
Camilo E. López https://orcid.org/0000-0003-4592-8614
César Augusto Medina Culma https://orcid.org/0000-0001-8342-5300
Laurent D. Noël https://orcid.org/0000-0002-0110-1423
Boris Szurek https://orcid.org/0000-0002-1808-7082
Carlos Andrés Zárate-Chaves https://orcid.org/0000-0002-5588-710X

Data availability

Publicly available datasets were analyzed in this study: Genomes from PXO99^A (GCF_000019585.2), MAI1 (GCF_003031365.1), and IAPAR 306 (GCF_000007165.1) were retrieved from NCBI. The promoter sequences obtained in this study are shown in Table S4, while RVD sequences for *Xanthomonas cassavae* TALEs are summarized in Table S5.

References

Anzalone AV, Koblan LW, Liu DR. 2020. Genome editing with CRISPR–Cas nucleases, base editors, transposases and prime editors. *Nature Biotechnology* **38**: 824–844.

Anzalone AV, Randolph PB, Davis JR, Sousa AA, Koblan LW, Levy JM, Chen PJ, Wilson C, Newby GA, Raguram A et al. 2019. Search-and-replace genome editing without double-strand breaks or donor DNA. *Nature* **576**: 149–157.

Aung K, Jiang Y, He SY. 2018. The role of water in plant–microbe interactions. *The Plant Journal* **93**: 771–780.

Banno S, Nishida K, Arazoe T, Mitsunobu H, Kondo A. 2018. Deaminase-mediated multiplex genome editing in *Escherichia coli*. *Nature Microbiology* **3**: 423–429.

Barrangou R, Fremaux C, Deveau H, Richards M, Boyaval P, Moineau S, Romero DA, Horvath P. 2007. CRISPR provides acquired resistance against viruses in prokaryotes. *Science* **315**: 1709–1712.

Bikard D, Jiang W, Samai P, Hochschild A, Zhang F, Marraffini LA. 2013. Programmable repression and activation of bacterial gene expression using an engineered CRISPR-Cas system. *Nucleic Acids Research* **41**: 7429–7437.

Boch J, Bonas U. 2010. *Xanthomonas* AvrBs3 family-type III effectors: discovery and function. *Annual Review of Phytopathology* **48**: 419–436.

Boch J, Scholze H, Schornack S, Landgraf A, Hahn S, Kay S, Lahaye T, Nickstadt A, Bonas U. 2009. Breaking the code of DNA binding specificity of TAL-type III effectors. *Science* **326**: 1509–1512.

Bredeson JV, Lyons JB, Prochnik SE, Wu GA, Ha CM, Edsinger-Gonzales E, Grimwood J, Schmutz J, Rabbi IY, Egesi C et al. 2016. Sequencing wild and cultivated cassava and related species reveals extensive interspecific hybridization and genetic diversity. *Nature Biotechnology* **34**: 562–570.

Breia R, Conde A, Badim H, Fortes AM, Gerós H, Granell A. 2021. Plant SWEETs: from sugar transport to plant–pathogen interaction and more unexpected physiological roles. *Plant Physiology* **186**: 836–852.

Brito LF, Schultenkämper K, Passaglia LMP, Wendisch VF. 2020. CRISPR interference-based gene repression in the plant growth promoter *Paenibacillus sonchi* genomovar Riograndensis SBR5. *Applied Microbiology and Biotechnology* **104**: 5095–5106.

Brouns SJJ, Jore MM, Lundgren M, Westra ER, Slijkhuis RJH, Snijders APL, Dickman MJ, Makarova KS, Koonin EV, van der Oost J. 2008. Small CRISPR RNAs guide antiviral defense in prokaryotes. *Science* **321**: 960–964.

Chin CS, Alexander DH, Marks P, Klammer AA, Drake J, Heiner C, Clum A, Copeland A, Huddleston J, Eichler EE et al. 2013. Nonhybrid, finished microbial genome assemblies from long-read SMRT sequencing data. *Nature Methods* **10**: 563–569.

Choi K-H, Schweizer HP. 2006. mini-Tn7 insertion in bacteria with single attTn7 sites: example *Pseudomonas aeruginosa*. *Nature Protocols* **1**: 153–161.

Cohn M, Bart RS, Shybut M, Dahlbeck D, Gomez M, Morbitzer R, Hou B-H, Frommer WB, Lahaye T, Staskawicz BJ. 2014. *Xanthomonas axonopodis* virulence is promoted by a transcription activator-like effector-mediated induction of a SWEET sugar transporter in cassava. *Molecular Plant–Microbe Interactions* **27**: 1186–1198.

Collias D, Beisel CL. 2021. CRISPR technologies and the search for the PAM-free nuclease. *Nature Communications* **12**: 555.

Cox KL, Meng F, Wilkins KE, Li F, Wang P, Booher NJ, Carpenter SCD, Chen L-Q, Zheng H, Gao X et al. 2017. TAL effector driven induction of a SWEET gene confers susceptibility to bacterial blight of cotton. *Nature Communications* **8**: 15588.

Cui L, Bikard D. 2016. Consequences of Cas9 cleavage in the chromosome of *Escherichia coli*. *Nucleic Acids Research* **44**: 4243–4251.

Cunnac S, Chakravarthy S, Kvitko BH, Russell AB, Martin GB, Collmer A. 2011. Genetic disassembly and combinatorial reassembly identify a minimal functional repertoire of type III effectors in Pseudomonas syringae. *Proceedings of the National Academy of Sciences, USA* **108**: 2975–2980.

Denancé N, Szurek B, Doyle EL, Lauber E, Fontaine-Bodin L, Carrère S, Guy E, Hajri A, Cerutti A, Boureau T et al. 2018. Two ancestral genes shaped the *Xanthomonas campestris* TAL effector gene repertoire. *New Phytologist* **219**: 391–407.

Ding W, Zhang Y, Shi S. 2020. Development and application of CRISPR/Cas in microbial biotechnology. *Frontiers in Bioengineering and Biotechnology* **8**: 711.

Doench JG, Hartenian E, Graham DB, Tothova Z, Hegde M, Smith I, Sullender M, Ebert BL, Xavier RJ, Root DE. 2014. Rational design of highly active sgRNAs for CRISPR-Cas9-mediated gene inactivation. *Nature Biotechnology* **32**: 1262–1267.

Ellis NA, Kim B, Tung J, Machner MP. 2021. A multiplex CRISPR interference tool for virulence gene interrogation in *Legionella pneumophila*. *Communications Biology* **4**: 157.

Erkes A, Reschke M, Boch J, Grau J. 2017. Evolution of transcription activator-like effectors in *Xanthomonas oryzae*. *Genome Biology and Evolution* **9**: 1599–1615.

Ferreira RM, de Oliveira ACP, Moreira LM, Belasque J, Gourbeyre E, Siguier P, Ferro MIT, Ferro JA, Chandler M, Varani AM. 2015. A TALE of transposition: Tn3-Like transposons play a major role in the spread of

pathogenicity determinants of *Xanthomonas citri* and other *Xanthomonads*. *mBio* 6: e02505-14.

Gasiunas G, Barrangou R, Horvath P, Siksnys V. 2012. Cas9-crRNA ribonucleoprotein complex mediates specific DNA cleavage for adaptive immunity in bacteria. *Proceedings of the National Academy of Sciences, USA* 109: E2579–E2586.

Gaudelli NM, Komor AC, Rees HA, Packer MS, Badran AH, Bryson DI, Liu DR. 2017. Programmable base editing of A•T to G•C in genomic DNA without DNA cleavage. *Nature* 551: 464–471.

Geißler R, Scholze H, Hahn S, Streubel J, Bonas U, Behrens S-E, Boch J. 2011. Transcriptional activators of human genes with programmable DNA-specificity. *PLoS ONE* 6: e19509.

Hsu PD, Scott DA, Weinstein JA, Ran FA, Konermann S, Agarwala V, Li Y, Fine EJ, Wu X, Shalem O et al. 2013. DNA targeting specificity of RNA-guided Cas9 nucleases. *Nature Biotechnology* 31: 827–832.

Hu Y, Zhang J, Jia H, Sosso D, Li T, Frommer WB, Yang B, White FF, Wang N, Jones JB. 2014. Lateral organ boundaries 1 is a disease susceptibility gene for citrus bacterial canker disease. *Proceedings of the National Academy of Sciences, USA* 111: E521–E529.

Hunt M, De SN, Otto TD, Parkhill J, Keane JA, Harris SR. 2015. Circlator: automated circularization of genome assemblies using long sequencing reads. *Genome Biology* 16: 294.

Ji Z, Ji C, Liu B, Zou L, Chen G, Yang B. 2016. Interfering TAL effectors of *Xanthomonas oryzae* neutralize R-gene-mediated plant disease resistance. *Nature Communications* 7: 13435.

Kay S, Boch J, Bonas U. 2005. Characterization of AvrBs3-like effectors from a Brassicaceae pathogen reveals virulence and avirulence activities and a protein with a novel repeat architecture. *Molecular Plant–Microbe Interactions* 18: 838–848.

Koren S, Walenz BP, Berlin K, Miller JR, Bergman NH, Phillippy AM. 2017. CANU: scalable and accurate long-read assembly via adaptive *k*-mer weighting and repeat separation. *Genome Research* 27: 722–736.

Kvitko BH, Park DH, Velásquez AC, Wei C-F, Russell AB, Martin GB, Schneider DJ, Collmer A. 2009. Deletions in the repertoire of *Pseudomonas syringae* pv. *tomato* DC3000 type III secretion effector genes reveal functional overlap among effectors. *PLoS Pathogens* 5: e1000388.

Larson MH, Gilbert LA, Wang X, Lim WA, Weissman JS, Qi LS. 2013. CRISPR interference (CRISPRi) for sequence-specific control of gene expression. *Nature Protocols* 8: 2180–2196.

Liu R, Liang L, Freed EF, Gill RT. 2021. Directed evolution of CRISPR/Cas systems for precise gene editing. *Trends in Biotechnology* 39: 262–273.

Mak AN-S, Bradley P, Cernadas RA, Bogdanove AJ, Stoddard BL. 2012. The crystal structure of TAL effector PthXo1 bound to its DNA target. *Science* 335: 716–719.

Moscou MJ, Bogdanove AJ. 2009. A simple cipher governs DNA recognition by TAL effectors. *Science* 326: 1501.

Pérez-Quintero AL, Rodriguez-R LM, Dereeper A, López Carrascal CE, Koebnik R, Szurek B, Cunnac S. 2013. An improved method for TAL effectors DNA-binding sites prediction reveals functional convergence in TAL repertoires of *Xanthomonas oryzae* strains. *PLoS ONE* 8: e68464.

Perez-Quintero AL, Szurek B. 2019. A decade decoded: spies and hackers in the history of TAL effectors research. *Annual Review of Phytopathology* 57: 459–481.

Peters JE, Craig NL. 2001. Tn7 recognizes transposition target structures associated with DNA replication using the DNA-binding protein TnsE. *Genes & Development* 15: 737–747.

Qi LS, Larson MH, Gilbert LA, Doudna JA, Weissman JS, Arkin AP, Lim WA. 2013. Repurposing CRISPR as an RNA-guided platform for sequence-specific control of gene expression. *Cell* 152: 1173–1183.

Read AC, Hutin M, Moscou MJ, Rinaldi FC, Bogdanove AJ. 2020. Cloning of the rice Xo1 resistance gene and interaction of the Xo1 protein with the defense-suppressing Xanthomonas effector Tal2h. *Molecular Plant–Microbe Interactions* 33: 1189–1195.

Read AC, Rinaldi F, Hutin M, He Y, Triplett L, Bogdanove AJ. 2016. Suppression of Xo1-mediated disease resistance in rice by a truncated, non-DNA-binding TAL effector of *Xanthomonas oryzae*. *Frontiers in Plant Science* 7: 1516.

Salzberg SL, Sommer DD, Schatz MC, Phillippy AM, Rabinowicz PD, Tsuge S, Furutani A, Ochiai H, Delcher AL, Kelley D et al. 2008. Genome sequence and rapid evolution of the rice pathogen *Xanthomonas oryzae pv. oryzae* PXO99A. *BMC Genomics* 9: 204.

Schandry N, Jacobs JM, Szurek B, Perez-Quintero AL. 2018. A cautionary TALE: how plant breeding may have favoured expanded TALE repertoires in *Xanthomonas*. *Molecular Plant Pathology* 19: 1297–1301.

Streubel J, Pesce C, Hutin M, Koebnik R, Boch J, Szurek B. 2013. Five phylogenetically close rice *SWEET* genes confer TAL effector-mediated susceptibility to *Xanthomonas oryzae* pv. *oryzae*. *New Phytologist* 200: 808–819.

Sugio A, Yang B, Zhu T, White FF. 2007. Two type III effector genes of *Xanthomonas oryzae* pv. *oryzae* control the induction of the host genes OsTFIIAγ1 and OsTFX1 during bacterial blight of rice. *Proceedings of the National Academy of Sciences, USA* 104: 10720–10725.

Tan SZ, Reisch CR, Prather KLJ. 2018. A robust CRISPR interference gene repression system in *Pseudomonas*. *Journal of Bacteriology* 200: e00575-17.

Wei C-F, Kvitko BH, Shimizu R, Crabill E, Alfano JR, Lin N-C, Martin GB, Huang H-C, Collmer A. 2007. A *Pseudomonas syringae* pv. *tomato* DC3000 mutant lacking the type III effector HopQ1-1 is able to cause disease in the model plant *Nicotiana benthamiana*. *The Plant Journal* 51: 32–46.

Xue J, Lu Z, Liu W, Wang S, Lu D, Wang X, He X. 2021. The genetic arms race between plant and *Xanthomonas*: lessons learned from TALE biology. *Science China Life Sciences* 64: 51–65.

Yuan M, Ke Y, Huang R, Ma L, Yang Z, Chu Z, Xiao J, Li X, Wang S. 2016. A host basal transcription factor is a key component for infection of rice by TALE-carrying bacteria. *eLife* 5: e19605.

Zárate-Chaves CA, Gómez de la Cruz D, Verdier V, López CE, Bernal A, Szurek B. 2021a. Cassava diseases caused by *Xanthomonas phaseoli* pv. *manihotis* and *Xanthomonas cassavae*. *Molecular Plant Pathology* 22: 1520–1537.

Zárate-Chaves CA, Osorio-Rodríguez D, Mora RE, Pérez-Quintero ÁL, Dereeper A, Restrepo S, López CE, Szurek B, Bernal A. 2021b. TAL effector repertoires of strains of *Xanthomonas phaseoli* pv. *manihotis* in commercial cassava crops reveal high diversity at the country scale. *Microorganisms* 9: 315.

Zhang R, Xu W, Shao S, Wang Q. 2021. Gene silencing through CRISPR interference in bacteria: current advances and future prospects. *Frontiers in Microbiology* 12: 635227.

Supporting Information

Additional Supporting Information may be found online in the Supporting Information section at the end of the article.

Fig. S1 MUSCLE alignment of 30 *Xanthomonas phaseoli* pv *manihotis* (*Xpm*) *tale* promoter regions shows two polymorphisms in positions 12th and 13th of the RBS CRISPR RNAs (crRNAs) for some *tale* genes.

Fig. S2 Alignment of *tale* promoter regions from the five tested *Xanthomonas* strains from different pathovars shows that target locus for RBS CRISPR RNA (crRNA) is highly conserved among them.

Fig. S3 Constructs used for single guide RNA (sgRNA) cloning and chromosomal insertion.

Fig. S4 Elements of the CRISPR interference (CRISPRi) platform and complementation plasmid.

Fig. S5 Mini-Tn7 transposon-mediated insertion of *dCas9* into the genome of *Xpm* does not induce changes in pathogen growth and virulence.

Fig. S6 *tale* gene knockdown in *Xpm* abolishes pathogen virulence.

New
Phytologist

Fig. S7 Identification of *Xanthomonas* spp. TALEs present in total protein extracts resolved by SDS-PAGE and detected by anti-TALE antibodies.

Fig. S8 *Xanthomonas cassavae* CRISPRi strain CFBP 4642-RBS shows reduced symptom development after infiltration at two different concentrations and time points in leaves of the cassava cultivar CM6438-14.

Fig. S9 Comprehensive one-to-one statistical *post hoc* comparisons.

Methods S1 Detailed methods and supplementary results.

Table S1 Microorganisms used in this study.

Table S2 Scale for scoring black rot symptoms and calculating disease index in *Brassica oleracea* var. *botrytis* cv *Clovis* (Vilmorin) leaves.

Table S3 Primers used in this study.

Table S4 Promoter region sequences of 31 *tale* genes extracted from the TALomes of 10 *Xanthomonas phaseoli* pv *manihotis* strains.

Table S5 TALE proteins from *Xanthomonas cassavae* strain CFBP 4642 obtained by Pacific Biosciences DNA sequencing.

Table S6 TALVEZ predictions of targeted cassava (*Manihot esculenta*) genes for TALE23$_{CFBP4642}$.

Please note: Wiley is not responsible for the content or functionality of any Supporting Information supplied by the authors. Any queries (other than missing material) should be directed to the *New Phytologist* Central Office.